# Ultrafast Slow-Light Tuning Beyond the Carrier Lifetime Using Photonic Crystal Waveguides

K. Kondo,[1] M. Shinkawa,[1,2] Y. Hamachi,[1,2] Y. Saito,[1,2] Y. Arita,[1,2] and T. Baba[1,2]

[1]*Department of Electrical and Computer Engineering, Yokohama National University, 79-5 Tokiwadai, Hodogayaku, Yokohama 240-8501, Japan*

[2]*Core Research for the Evolutional Science and Technology, Japan Science and Technology Agency, 5 Sanbancho, Chiyodaku, Tokyo 102-0075, Japan*

(Received 20 August 2012; published 30 January 2013)

We demonstrate ultrafast delay tuning of a slow-light pulse with a response time $<10$ ps. This is achieved using two types of slow light: dispersion-compensated slow light for the signal pulse, and low-dispersion slow light to enhance nonlinear effects of the control pulse. These two types of slow light are generated simultaneously in Si lattice-shifted photonic crystal waveguides, arising from flat and straight photonic bands, respectively. The control pulse blueshifts the signal pulse spectrum, through dynamic tuning caused by the plasma effect of two-photon-absorption-induced carriers. This changes the delay by up to 10 ps only when the two pulses overlap within the waveguide and enables ultrafast tuning that is not limited by the carrier lifetime. Using this, we succeeded in tuning the delay of one target pulse within a pulse train with 12 ps intervals.

DOI: 10.1103/PhysRevLett.110.053902 PACS numbers: 42.70.Qs, 42.25.Bs, 42.65.Re, 42.82.−m

Photonic crystal waveguides (PCWs) generate slow light because of the small slope of the photonic band $d\omega/dk$ [1]. Slow light enhances light-matter interactions and enables the miniaturization of photonic devices. Some modified PCWs produce a straight band, which we refer to as a low-dispersion (LD) slow-light band [2–4]. This compresses the propagating pulse in space and enhances nonlinearities [5–7]. We have proposed and studied lattice-shifted PCW (LSPCW) as such a modified PCW and observed large two-photon absorption (TPA), self-phase modulation, and four-wave mixing (FWM) in Si-based devices at wavelengths $\lambda \sim 1550$ nm [5,7]. For large lattice shifts, a flat band also appears at another frequency, which generates narrow-band slow-light, giving a long delay. When an index chirp is formed along the LSPCW, the flat-band frequency is shifted with position and its delay is averaged. This also allows short pulses to propagate as dispersion-compensated (DC) slow light whose bandwidth and delay are controlled by the chirp range [8]. Tunable delays $<100$ ps have been obtained by the thermo-optic (TO) effect, while its switching response time is as long as the 10 $\mu$s order [9,10]. In this Letter, we report that the two types of slow light, LD and DC, are generated simultaneously in the LSPCW, and that ultrafast delay tuning of the DC slow light (signal pulse) is possible by using the TPA-induced carrier plasma effect, which is enhanced by the LD slow light (control pulse). The carrier plasma effect is much faster than the TO effect. However, its response is usually limited by the carrier lifetime of sub-ns to ns order and is still too slow for many applications. Our method breaks this limit and allows a response time $<10$ ps. Even though the tuning range is narrower than that of the TO effect, such a fast response is applicable to the retiming of high-speed optical signals, for example.

Let us explain the principle in more detail. Figure 1 summarizes the fabricated LSPCW, index chirp in Si and calculated bands (see Supplemental Material for the device structure, fabrication, and band calculation [11]). The chirp, preformed by, for example, sloped heating, shifts the band frequency but does not change the band shape significantly provided that the chirp range is small. Therefore, for pulses with a spectrum overlapping with and narrower than the LD band, the same low-group velocity and low dispersion are maintained even with the chirp. On the other hand, the flat band (blue line) shifted by the chirp gives an averaged delay in the DC band, and the total group velocity dispersion (GVD) is canceled by the opposite GVD characteristics sandwiching the flat band. A larger chirp expands the DC band while reducing the averaged delay. When the incident LD pulses are intensified, the TPA-induced carrier plasma effect occurs. Since the pulse decays during the propagation owing to any losses, the carrier plasma effect is also sloped. This modifies the chirp profile and hence the delay of the DC pulse. Now we use the condition that the LD pulse propagates faster than the DC pulse. If the LD pulse is incident first and generates carriers, the delay changes simply, as mentioned above, within the carrier lifetime (we call it the *static tuning*). On the other hand, if their order is reversed and they overlap temporarily in the waveguide, carriers generated within the overlap duration cause adiabatic wavelength conversion [12–17] in the DC pulse (*dynamic tuning*) simultaneously with modifying the chirp. This results in a larger change of the delay. So far, the delay tuning through the wavelength conversion (FWM) and GVD in fibers has been reported [18]. Our method, on the other hand, completely achieves this on a chip based on the dynamic tuning and slow-light engineering. It does not require a large $\chi^{(3)}$ but an efficient

 

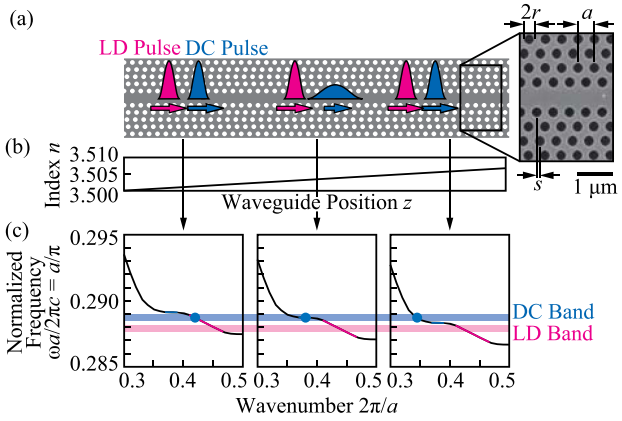


FIG. 1 (color online). LSPCW and slow light. (a) Scanning electron micrograph of the device fabricated by CMOS-compatible process and schematic of the two slow-light pulses. (b) Index chirp in Si. (c) Calculated photonic bands for transverse-electric-like (TE-like) polarization, assuming the index chirp in (b). Blue dots on bands indicate that the GVD of DC slow-light changes from positive (left), zero (center), to negative (right).

carrier plasma effect, and it achieves a much higher efficiency. Moreover, the ultrafast delay tuning is possible, because the overlap duration is independent of the carrier lifetime but can be preset by the device length and also controlled externally by the incident timing of the two pulses.

In the following, we show some experimental results. Figure 2 shows the measured transmission and group delay spectra of fabricated LSPCW, where the chirp was not formed intentionally but some nonuniformity in the device might form a slight chirp. At the DC band, a dip and peak appear in these spectra, respectively. The dip is because of losses enhanced by the slow-light effect at the DC band. The LD band also appears on the long wavelength side. In the delay tuning experiment, we preformed the index chirp by heating the center of the LSPCW so that the delay peak at the DC band is moderated further. We generated a 4.9 ps

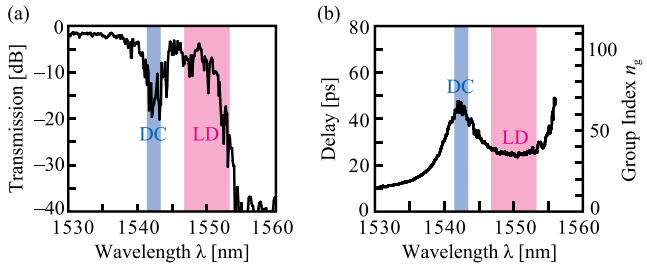


FIG. 2 (color online). Light propagation characteristics of the fabricated LSPCW for TE-like polarization. (a) Transmission spectrum, normalized by that of a Si wire waveguide with the same length. (b) Group delay and group index ($n_g$) spectra with a wavelength resolution of 0.6 nm. $n_g$ at the delay peak and at the center of LD band are 65 and 35, respectively.

wide signal pulse and 2.4 ps wide control pulse at the DC and LD bands, respectively, and launched on the LSPCW after tuning the incident timing. Then, we measured the waveform and spectrum of the output signal pulse (see Supplemental Material for the detail of the measurement [11]). Figure 3(a) shows the waveforms of the signal pulse at different incident timings of the control pulse, $\Delta t_c$, while Fig. 3(b) plots the temporal peaks of the waveforms that correspond to the delay of the signal pulse, $\Delta t_s$. We can see two regimes: (i) at $\Delta t_c < -1$ ps, a small positive $\Delta t_s$ occurs, and its dependence on $\Delta t_c$ is small; and (ii) at $-1 \leq \Delta t_c \leq 9$ ps, $\Delta t_s$ decreases significantly and depends strongly on $\Delta t_c$. In both regimes, the pulse shape is almost maintained, although slight distortion and splitting are observed in (ii).

In regime (i), small $\Delta t_s$ is observed even at $\Delta t_c < -100$ ps. Since the control pulse already exits from the LSPCW when the signal pulse enters, the delay in (i) should be because of the TPA-induced carriers already existing and remaining in the LSPCW. This is confirmed from the behavior of $\Delta t_s$ at different signal wavelengths and the change of the output signal pulse spectrum, as shown in Fig. 4. The delay in (i) changes with the wavelength and switches from positive to negative on the long wavelength side. The output spectrum [$A$ corresponds to (i) in Fig. 4(b)] shows little changes with and without the control pulse; only the spectral intensity decreases with the control pulse because of the free carrier absorption. To summarize these results, the delay versus spectral peak characteristics are plotted with and without the control pulse as open and closed circles, respectively, at various input wavelengths, as shown in Fig. 5(a). Here, closed circles are lying on the original group delay spectrum (solid line), while open circles should be on the changed group delay spectrum (the dashed line can be drawn so as to pass through open circles). It is seen that, with the control pulse, the delay spectrum blueshifts and expands slightly, while the signal spectrum does not change at all. This blueshift makes $\Delta t_s$ positive at shorter wavelengths and negative at longer wavelengths. Let us go back to Fig. 3(b). $|\Delta t_c|$ that reduces $\Delta t_s$ to $1/e$ of its maximum should give the carrier lifetime. It is estimated to be 120 ps, which is similar to 100 ps in a Si photonic crystal nanocavity [19], explained to be dominated by carrier diffusion.

In regime (ii), on the other hand, a large negative $\Delta t_s$ up to $-10$ ps occurs within the narrow range of $\Delta t_c$ in Fig. 3, but it turns positive on the long wavelength side in Fig. 4(a). The behaviors arise from the blueshift in the signal spectrum [$B$ corresponds to (ii) in Fig. 4(b)]. The same summary as for (i) can be plotted for (ii), as shown in Fig. 5(b). In contrast to (a), the group delay spectrum does not change, while circular plots blueshift along the group delay spectrum. One possible reason for the blueshift is cross-phase modulation, which occurs when the control pulse overtakes the signal pulse. However, that caused in

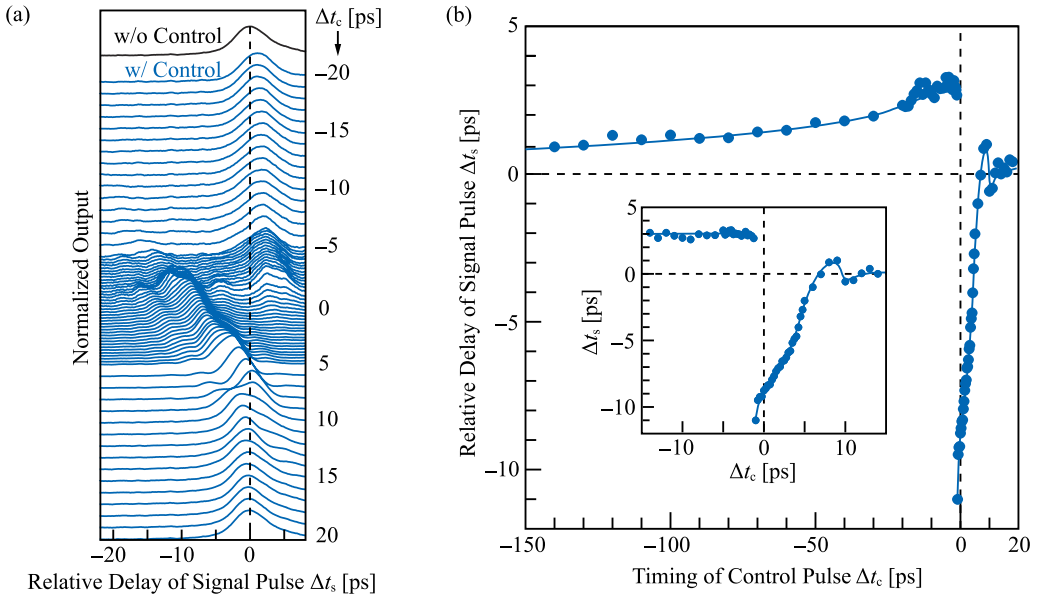


FIG. 3 (color online). Observed delay tuning. (a) Cross-correlation traces of output signal pulse at different $\Delta t_c$. Here, $\Delta t_c = 0$ corresponds to the control and signal pulses being incident simultaneously, and $\Delta t_c > 0$ is when the control pulse is incident later. For the delay $\Delta t_s$ of the signal pulse, the pulse peak without the control pulse is used for reference. (b) $\Delta t_s$ versus $\Delta t_c$ characteristics.

terms of $\chi^{(3)}$ is fundamentally small, and its spectral red- and blueshifts occurring at the rising- and falling-edges of the control pulse, respectively, almost cancel each other. Therefore, the main reason should be the dynamic tuning. At the moment that the two0 pulses overlap, the signal pulse spectrum blueshifts together with the delay spectrum, but this does not change the delay of the pulse. Rather, the delay changes when the signal pulse goes forward slightly and enters the next section whose delay spectrum is not yet changed by the dynamic tuning; the delay decreases (increases) when the pulse wavelength is shorter (longer) than the delay peak. Repeating this process finally gives a large negative (positive) $\Delta t_s$, the blueshift in the signal pulse, and no explicit change of the group delay spectrum, as depicted in Fig. 5(b). These effects are maximized when the two pulses overlap near the input end of the LSPCW where the control pulse has the maximum power. In fact, the largest $\Delta t_s$ in (ii) occurs within the gray

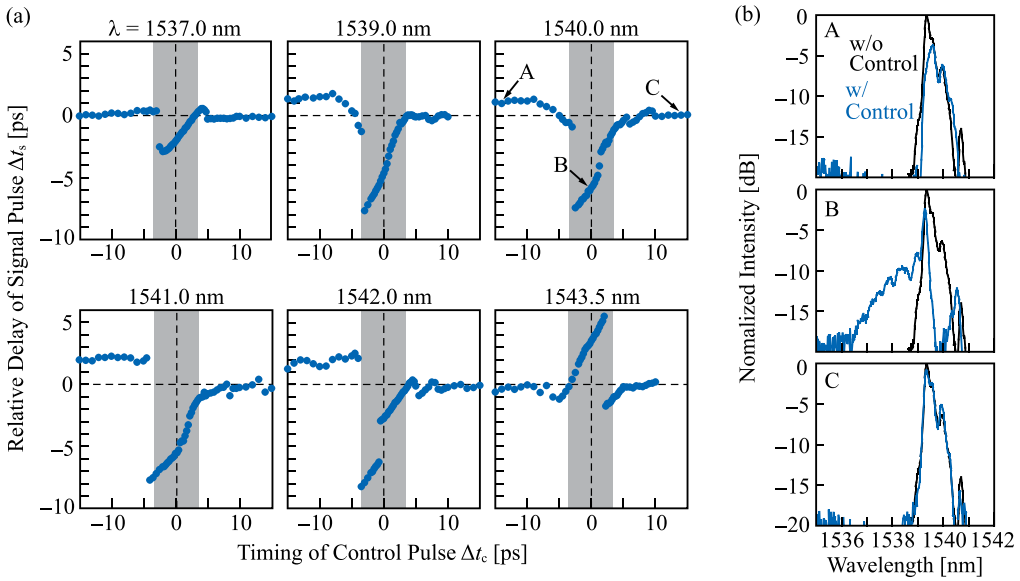


FIG. 4 (color online). Dependence of delay tuning on signal pulse wavelength. (a) $\Delta t_s$ versus $\Delta t_c$ characteristics. Gray zones depict the timing that the control and signal pulses overlap at the input end. (b) Spectra of the output signal pulse. A–C correspond to the points indicated in (a).

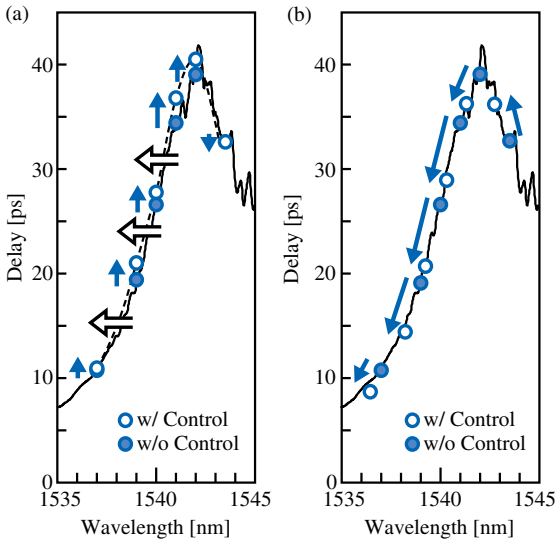


FIG. 5 (color online). Summary of the delay and spectrum of the signal pulse with and without control pulse (circles) and group delay spectrum of LSPCW with preformed index chirp (solid line). Closed and open arrows suggest the behaviors of signal pulse and group delay spectrum, respectively. (a) Static tuning in regime (i). Open circles are plotted for $\Delta t_c = -10$ ps. Dashed line is drawn so as to pass through open circles. (b) Dynamic tuning in regime (ii). Open circles are plotted for $\Delta t_c = 0$ ps.

zone satisfying this condition, as shown in Fig. 4(a). Since the two pulses have different temporal widths, the overlap is partial and the blueshift is nonuniform, leading to some distortion and splitting in the pulse. When the control pulse is incident too late, it cannot overtake the signal pulse in the LSPCW. Therefore, the delay and spectrum in $C$ of Fig. 4 do not change at $\Delta t_c > 10$ ps. It is seen from these considerations that the response time can be shortened by shortening the LSPCW and the overlapping duration. Moreover, $|\Delta t_s|$ can be increased by intensifying the control pulse. In fact, we observed that the maximum $|\Delta t_s|$ is tuned in the range of 3.5–11 ps when the intensity is changed by 5 dB. We can also increase $|\Delta t_s|$ by broadening the control pulse and elongating the LSPCW, while in this case, the switching becomes slower.

By using the fast response, we can tune the delay of one target pulse in a pulse train with an interval over 10 ps. To demonstrate this, we prepared a train of four pulses with a $12 \pm 1$ ps interval using a Si photonics circuit (see Supplemental Material for the details of this circuit [11]). The circuit is inserted in the optical path for producing the signal pulse, and the delay tuning is observed, as shown in Fig. 6. Here, intensities of all pulses are normalized so that the delay is more visible. (If they are not normalized, the intensity of the delayed pulse is reduced by ~20% because of the free carrier absorption and pulse distortion.) The delay of the target pulse is reduced by 2.0–2.6 ps using regime (ii) by adjusting $\Delta t_c$. The delay of the pulse next to the target increases slightly ($< 1$ ps) because of regime (i).

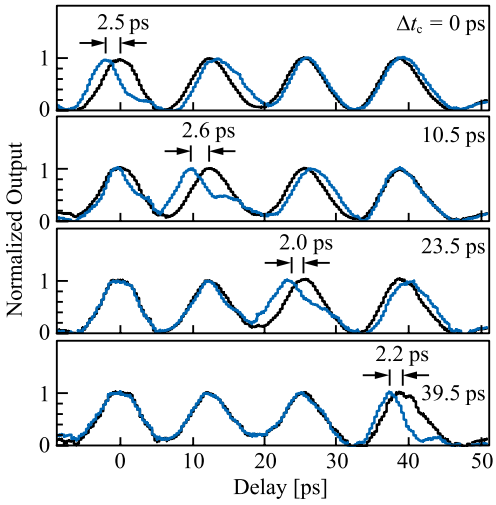


FIG. 6 (color online). Selective delay tuning of one target pulse in a pulse train. Light and dark colored lines show normalized correlation traces of output pulses observed with and without control pulse, respectively. The basis of the lateral axis is the same as for $\Delta t_c$. Pulse position is evaluated as the center between the half maxima.

This increase can be minimized by optimizing the wavelength, as can be seen in Fig. 4(a). Meanwhile, the change of the delay in regime (ii) suggests that, when the signal pulse is incident behind and ahead of a reference timing [center of the gray zone in Fig. 4(a)], its delay decreases and increases, respectively, and minimizes the time lag from the reference. This means that it can be applied for the retiming of a disordered signal pulse train when the control pulse is continuously incident as a clock.

In conclusion, we succeeded in tuning the delay of the signal pulse all optically using two types of slow light in the LSPCW. Here, the TPA-induced carrier plasma effect gives rise to the dynamic tuning, resulting in the ultrafast delay tuning that is not limited by the carrier lifetime but instead by the device length and the incident timing of the control pulse. Integrating the LSPCW with heaters and $p$-$n$ diodes, using a CMOS-compatible process, we can control externally not only the delay characteristics but also the target wavelength and dispersion [10]. Therefore, flexible delay tuning of ps pulses will be possible using an all in-line setup, which is suitable for practical applications such as the retiming of optical signals.

This work was partly supported by the FIRST Program of Japan Society for the Promotion of Science.

[1] T. Baba, Nat. Photonics **2**, 465 (2008).
[2] L. H. Frandsen, A. V. Lavrinenko, J. Fage-Pedersen, and P. I. Borel, Opt. Express **14**, 9444 (2006).
[3] S. Kubo, D. Mori, and T. Baba, Opt. Lett. **32**, 2981 (2007).
[4] J. Li, T. P. White, L. O'Faolain, A. Gomez-Iglesias, and T. F. Krauss, Opt. Express **16**, 6227 (2008).

[5] Y. Hamachi, S. Kubo, and T. Baba, Opt. Lett. **34**, 1072 (2009).
[6] C. Monat, M. Ebnali-Heidari, C. Grellet, B. Corcoran, B. J. Egglenton, T. P. White, L. O'Faolain, J. Li, and T. F. Krauss, Opt. Express **18**, 22 915 (2010).
[7] M. Shinkawa, N. Ishikura, Y. Hama, K. Suzuki, and T. Baba, Opt. Express **19**, 22 208 (2011).
[8] D. Mori and T. Baba, Opt. Express **13**, 9398 (2005).
[9] N. Ishikura, T. Baba, E. Kuramochi, and M. Notomi, Opt. Express **19**, 24102 (2011).
[10] N. Ishikura, R. Hosoi, R. Hayakawa, T. Tamanuki, M. Shinkawa, and T. Baba, Appl. Phys. Lett. **100**, 221110 (2012).
[11] See Supplemental Material at http://link.aps.org/supplemental/10.1103/PhysRevLett.110.053902 for details of devices, band calculation, measurement setup, and a supplemental device used for the final experiment.
[12] M. F. Yanik and S. Fan, Phys. Rev. Lett. **92**, 083901 (2004).
[13] M. Notomi and S. Mitsugi, Phys. Rev. A **73**, 051803 (2006).
[14] S. F. Preble, Q. Xu, and M. Lipson, Nat. Photonics **1**, 293 (2007).
[15] J. Upham, Y. Tanaka, T. Asano, and S. Noda, Appl. Phys. Express **3**, 062001 (2010).
[16] Y. Saito and T. Baba, Opt. Express **18**, 17141 (2010).
[17] D. M. Beggs, T. F. Krauss, L. Kuipers, and T. Kampfrath, Phys. Rev. Lett. **108**, 033902 (2012).
[18] Y. Dai, X. Chen, Y. Okawachi, A. C. Turner-Foster, M. A. Foster, M. Lipson, A. L. Gaeta, and C. Xu, Opt. Express **17**, 7004 (2009).
[19] T. Tanabe, M. Notomi, H. Taniyama, and E. Kuramochi, Phys. Rev. Lett. **102**, 043907 (2009).